

Gratings in indium oxide film overlayers on ion-exchanged waveguides by excimer laser micromachining

S. Pissadakis,^{a)} L. Reekie,^{b)} M. N. Zervas, and J. S. Wilkinson
Optoelectronics Research Centre, University of Southampton, SO17 1BJ, Southampton, United Kingdom

G. Kiriakidis
FO.R.T.H-IESL, Materials Group, P.O. Box 1527, Heraklion 71 110, Crete, Greece

(Received 17 August 2000; accepted for publication 4 December 2000)

Relief Bragg gratings were imprinted by 248 nm interferometric excimer laser ablation on potassium ion-exchanged channel waveguides in BK-7 glass overlaid with a thin high-index InO_x film. Using five pulses of energy density 60 mJ/cm^2 , a spectral transmittance notch of depth 66% and $\Delta\lambda_{\text{FWHM}} < 0.1 \text{ nm}$ was obtained at 1547 nm in the TE polarization for a waveguide having a nominal width of $8 \mu\text{m}$ and a 135-nm-thick InO_x overlayer. In waveguides coated with 100 nm InO_x , with widths increasing from 3 to $8 \mu\text{m}$, the reflection wavelength shifted by $0.12 \text{ nm}/\mu\text{m}$ and the reflectivity increased monotonically. © 2001 American Institute of Physics.
 [DOI: 10.1063/1.1345836]

Waveguide gratings are potentially important components in integrated optical circuits, providing signal filtering and routing with high extinction ratio, while allowing dense integration, robustness and stability. Bragg gratings were realized in planar waveguides in the 1970's¹ and have since been used extensively in line-narrowing semiconductor lasers. Recently, research into photosensitive^{2,3} and relief^{4,5} gratings has intensified due to renewed interest in integrated optical devices using alternative materials for telecommunications. Relief gratings may readily be applied to the majority of waveguide materials without requiring special photosensitive materials. This increases the design flexibility for the realization of high performance waveguide grating devices based on such alternative materials and optical configurations. Additionally, the application of excimer lasers to the fine machining of optical materials has recently been intensively investigated. Interferometric laser ablation has the potential for realizing strong gratings in compact waveguide devices, with the advantages of flexibility of wavelength selection and minimization of the number of process steps. We have recently demonstrated such reflection gratings at wavelengths near 1300 nm, directly written in thallium ion-exchanged glass waveguides by interferometric laser ablation at 193 nm.⁶ However, the exposure caused substantial damage to the waveguides, resulting in significant broadband losses. Nevertheless, interferometric excimer laser ablation is a flexible, simple and reliable relief grating patterning method, which has been used in the past for the imprinting of high-quality submicron relief gratings in thin oxide films.⁷ Bragg relief gratings have also been written by e-beam lithography and etching of titanium diffused waveguides in lithium niobate overlaid with a thin silicon film to enhance modal overlap with the grating.⁸

In this letter we present waveguide reflection submicron

relief gratings on multilayer waveguides operating near 1550 nm, fabricated by interferometric excimer laser ablation at 248 nm. The devices consisted of monomode potassium ion-exchanged channel waveguides in BK-7 glass overlaid for part of their length with a thin sputtered indium oxide (InO_x) film in which the gratings were written, as shown in Fig. 1. The refractive index of the deposited layer ($n \approx 1.7-1.8$) is significantly higher than the maximum refractive index of the diffused channel waveguide, causing the optical fields to be drawn up to the surface and interact strongly with the film.⁹ The thickness of the overlayer is chosen so that it is below cutoff and, therefore, it does not itself form a waveguide in the wavelength region of interest. Indium oxide was chosen as it may be machined using low energy densities, avoiding damage to the underlying ion-exchanged region. Light from a single-mode telecommunications fiber, butt coupled to the polished end face, excites the mode of the uncoated input section of the waveguide (A) and crosses the transition into the coated region (B). The modal intensity distribution in the coated region is drawn up to the surface by the high index film, as shown schematically in Fig. 1, resulting in larger overlap and increased sensitivity to surface perturbations. The thickness of the overlayer is ideally chosen to be small enough so that the coated waveguide is monomode and the scattering losses at the transitions are low. If a relief or photorefractive grating is recorded in the thin film over-

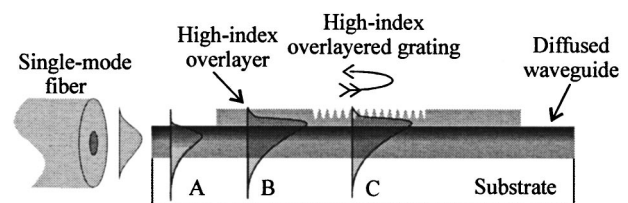


FIG. 1. Schematic representation of a high-index overlayer grating on an ion-exchanged waveguide. (A) propagating mode in uncoated region, (B) mode enhancement in the high-index overlaid region, (C) interaction of the enhanced mode with the high-index grating corrugation.

^{a)}Electronic mail: sp1@orc.soton.ac.uk

^{b)}Current address: JDS Uniphase Pty. Ltd., 4 Byfield Street, North Ryde, NSW 2113, Australia.

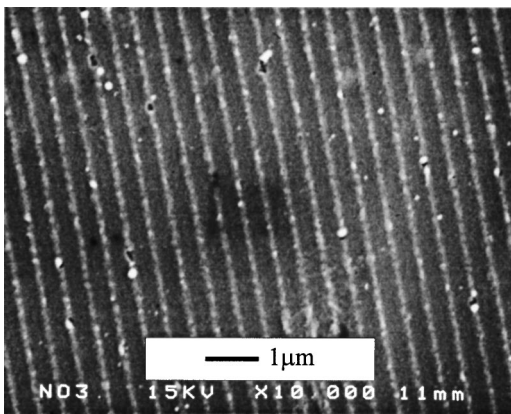


FIG. 2. Grating ablated in a 100-nm-thick InO_x film using 20 pulses of 45 mJ/cm^2 energy density.

layer (C) the field enhancement at the surface provides for strong interaction of the guided field with the grating.

Waveguides were fabricated by ion exchange in two BK-7 glass substrates in molten potassium nitrate through aluminum mask openings ranging from 3 to 8 μm , at 400 $^\circ\text{C}$ for 11 h.¹⁰ Polycrystalline indium oxide thin films, one of thickness 100 nm and one of thickness 135 nm, were sputtered on two waveguide chips using dc-magnetron sputtering in a 100% O_2 atmosphere to cover a 25 mm length in the center of the 40-mm-long waveguides. The overlaid waveguides were exposed to a high-contrast UV fringe pattern with period of 514.3 nm using the three-mirror interferometer described previously.⁶ The spatial distribution of the laser output was homogenized during recording using a rotating fused silica plate. Gratings of 16 mm length were produced on each set of waveguides by exposure to an average pulse energy density of 45–60 mJ/cm^2 using between 5 and 100 pulses. A scanning electron micrograph of a grating ablated in a 100-nm-thick InO_x film using 20 pulses of energy density 45 mJ/cm^2 is shown in Fig. 2.

Waveguide transmission spectra were obtained before InO_x deposition and after grating micromachining. Broadband amplified spontaneous emission from an erbium-doped fiber amplifier was coupled into each waveguide in turn using a monomode fiber. The waveguide output was collected by two $\times 10$ microscope objective lenses and an intermediate IR polarizer and launched into a multi-mode fiber coupled to an optical spectrum analyzer. The polarized transmission spectra for the waveguides were found by normalizing these spectra to that obtained with the monomode fiber butted directly to the multi-mode fiber. Reflection spectra were obtained using a fiber coupler at the input. The transmission losses of the waveguides before deposition of the InO_x films, including input fiber coupling losses, were less than 3 dB for both polarizations.

The transmission and reflection spectra for the TE polarization of an 8- μm -wide channel waveguide overlaid with a 135-nm-thick InO_x film supporting a grating ablated using five pulses of energy density 60 mJ/cm^2 are shown in Fig. 3. The average grating depth was estimated to be approximately 20 nm by atomic force microscope measurements. The transmission spectrum shows a broadband loss of about 4 dB, mainly due to fiber-waveguide coupling loss, including the transition losses between the coated and uncoated wave-

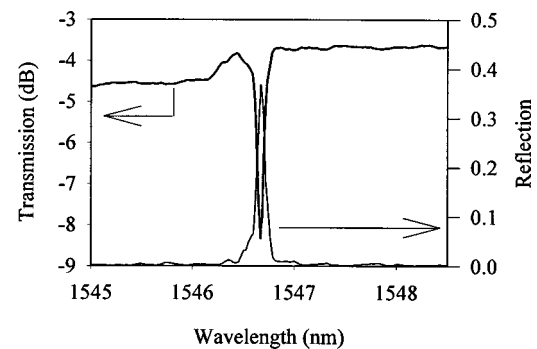


FIG. 3. Transmission (thick line) and reflection (thin line) spectra for an 8- μm -wide channel waveguide overlaid with 135-nm-thick InO_x film.

guide regions and propagation losses in the overlayer. The grating transmission showed a clear notch at 1546.7 nm with a depth of approximately 4.7 dB (66%) and a bandwidth at full width at half maximum power ($\Delta\lambda_{\text{FWHM}}$) of 0.08 nm. At wavelengths shorter than the Bragg wavelength the transmission spectrum shows an increased broadband loss, which is attributed to coupling to radiation modes. The insertion loss of the waveguide overlayer clearly remained low even after UV exposure of the film. Exposures with higher energy densities or a larger number of pulses resulted in significantly greater absorption loss and weaker grating strengths. Annealing of the waveguide chip up to 250 $^\circ\text{C}$ for 2 h in an oxygen atmosphere reduced the loss further by almost 1 dB. The reflection spectrum shows that reflected power is strongly coupled into the backward-traveling waveguide mode at 1546.7 nm. However, the grating strength in reflection is reduced to approximately 38% due to the additional background losses. No detectable grating response was observed for the TM polarization in reflection or transmission for a broadband of inspection over the amplified spontaneous emission spectrum of the erbium-doped fiber amplifier from 1520 to 1580 nm. Simulations using the beam propagation method show that the phase-matching wavelength for reflection in the TM polarization is expected to be of order 0.4 nm shorter than for TE polarization. Due to the presence of the high index film on the waveguide surface, the electromagnetic boundary conditions yield much greater intensity at the surface of the indium oxide film for the TE than for the TM polarization.⁹ In the present case the grating coupling constant for the TM polarization was calculated to be 3.75 times smaller than that for the TE polarization, resulting in a grating of predicted reflectivity no greater than 0.4 dB. Imperfections in the grating reduce the peak reflectivity further rendering this reflection immeasurable in comparison with spectral noise in the waveguide measurements.

Figure 4(a) shows the reflection spectra for waveguides with ion-exchange mask widths from 3 to 8 μm , coated with 100 nm InO_x and exposed to 20 pulses of energy density 60 mJ/cm^2 . Figure 4(b) summarizes these data by showing the reflection wavelength and peak reflectivity plotted against ion-exchange mask width. There is a near-linear dependence of the Bragg grating wavelength on the waveguide width, exhibiting a slope of 0.12 nm/ μm width change over this range. The grating strength in reflection increased from 3.0% and 14.8% for the same range of channels. The increase of grating reflectivity with the waveguide width is

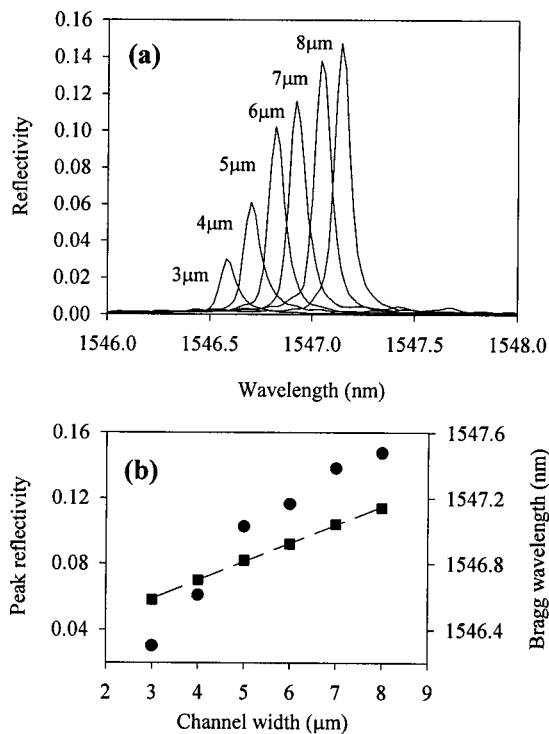


FIG. 4. (a) Grating reflection spectra and (b) peak reflectivity (circles) and Bragg wavelength (squares) vs waveguide width, for the TE polarization for waveguides overlaid with a 100-nm-thick InO_x film exposed to 20 pulses of energy density 60 mJ/cm^2 .

attributed to the greater confinement of the guiding mode closer to the surface of the waveguide channel, resulting in stronger interaction with the grating corrugation. Grating strengths up to 20 dB, accompanied by higher transmission losses, have also been observed in Ta_2O_5 overlaid devices and further details and comparative data will be presented elsewhere.

In conclusion, relief Bragg reflection gratings have been micromachined by 248 nm interferometric excimer laser ablation on potassium ion-exchanged channel waveguides in BK-7 glass overlaid with a thin high-index InO_x film. Using five pulses of energy density 60 mJ/cm^2 , a narrowband spectral transmittance notch of at least 66% and $\Delta\lambda_{\text{FWHM}} < 0.1 \text{ nm}$ was obtained at 1547 nm in the TE polarization for a waveguide having a nominal width of $8 \mu\text{m}$ and a 135-nm-thick InO_x overlayer. In waveguides coated with 100 nm InO_x , with widths increasing from 3 to $8 \mu\text{m}$, the reflection wavelength shifted by $0.12 \text{ nm}/\mu\text{m}$ and the reflectivity increased monotonically. Low-loss, polarization insensitive devices based on high-index overlaid waveguide gratings may be used for gain flattening or for wavelength add-drop applications. Further optimization of the device is directed towards the reduction of the UV-induced losses, and control of polarization sensitivity through optimization of overlayer film thickness.

- ¹D. C. Flanders, H. Kogelnik, R. V. Schmidt, and C. V. Shank, *Appl. Phys. Lett.* **24**, 194 (1974).
- ²D. F. Geraghty, D. Provenzano, W. K. Marshall, S. Honkanen, A. Yariv, and N. Peyghambarian, *Electron. Lett.* **35**, 585 (1999).
- ³M. Ibsen, J. Hubner, J. E. Pedersen, R. Kromann, L.-U. A. Andersen, and M. Kristensen, *Electron. Lett.* **32**, 2233 (1996).
- ⁴J. E. Roman and K. A. Winick, *Appl. Phys. Lett.* **61**, 2744 (1992).
- ⁵R. Adar, C. H. Henry, R. C. Kistler, and R. F. Kazarinov, *Appl. Phys. Lett.* **60**, 1779 (1992).
- ⁶S. Pissadakis, L. Reekie, M. Hempstead, M. N. Zervas, and J. S. Wilkinson, *Appl. Surf. Sci.* **153**, 200 (2000).
- ⁷S. Pissadakis, L. Reekie, J. S. Wilkinson, and G. Kiriakidis, *Proc. Conference on Lasers and Electro-Optics, Europe, Nice, France, 2000*, CWF50.
- ⁸C. P. Hessel and R. V. Ramaswamy, *IEEE Photonics Technol. Lett.* **9**, 636 (1997).
- ⁹G. R. Quigley, R. D. Harris, and J. S. Wilkinson, *Appl. Opt.* **38**, 6036 (1999).
- ¹⁰T. Feuchter, E. K. Mwarania, J. Wang, L. Reekie, and J. S. Wilkinson, *IEEE Photonics Technol. Lett.* **4**, 542 (1992).